DOI: 10.1002/anie.201409047

Solvation Dynamics

Solvation Dynamics of a Single Water Molecule Probed by Infrared Spectra—Theory Meets Experiment**

Matthias Wohlgemuth, Mitsuhiko Miyazaki, Martin Weiler, Makoto Sakai, Otto Dopfer, Masaaki Fujii,* and Roland Mitrić**

Abstract: *The dynamics and energetics of water at interfaces or in biological systems plays a fundamental role in all solvation and biological phenomena in aqueous solution. In particular, the migration of water molecules is the first step that controls the overall process in the time domain. Experimentally, the dynamics of individual water molecules is nearly impossible to follow in solution, because signals from molecules in heterogeneous environments overlap. Although molecular dynamics simulations do not have this restriction, there is a lack of experimental data to validate the calculated dynamics. Here, we demonstrate a new strategy, in which the calculated dynamics are verified by measured time-resolved infrared spectra. The coexistence of fast and slow migrations of water molecules around a CONH peptide linkage is revealed for a model system representative of a hydrate peptide.*

The fruitful interplay between theory and experiment is a major driving force for significant progress in physical chemistry and molecular physics. For example, molecular clusters, in which molecules interact by weak intermolecular forces such as hydrogen bonding and van der Waals forces, have been studied as models for solvation structures since the late 1970s.[1] However, their structures were mostly investigated independently by quantum chemical calculations and spectroscopy, and the conclusions were sometimes unrealistic from today's point of view.[2] Such structural studies experienced "a quantum leap" in the 1990s, when spectroscopists and theoreticians started collaborations. Spectroscopists recorded infrared (IR) spectra with novel high-power IR lasers, and theoreticians in turn suggested various possible cluster structures. Comparison between the spectral signatures in the measured and computed IR spectra then provided definite evidence as to which structure was observed.[3] Nowadays, this combined approach is the de facto standard in the cluster field and has revealed macroscopic properties associated with molecular parameters, such as the structure of bulk water from hydrogen-bonded networks in water clusters[4] and the photostability of DNA bases in their gas-phase clusters.[5]

What is the current situation for the chemical reaction and solvation *dynamics* in molecular clusters? Ultrafast laser experiments measure the time evolution of reaction products not only by simple pump–probe techniques but also by various sophisticated time-resolved laser methods, such as time-resolved photoelectron spectroscopy.[6] These studies mainly focus on the dissociation or the change in the electronic structure of molecules and clusters, because of the inherently low-energy resolution of femtosecond laser pulses, which is limited by the Heisenberg uncertainty principle. Thus, the experimental interest has focused on the assignment of reaction fragments and the evolution of molecular electronic states during the reaction. These are

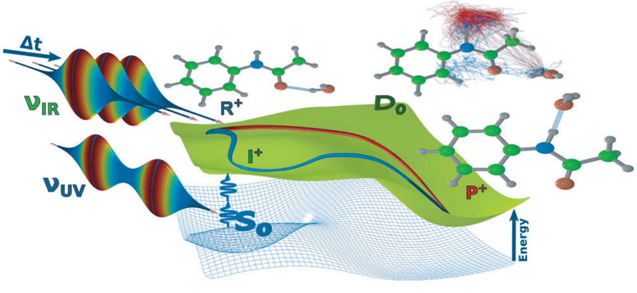

Figure 1. Scheme illustrating the experimental pump–probe procedure and dynamic time evolution after the ionization of the *trans*-acetanilide–water (AA–W) cluster. The CO-bound isomer is ionized by size- and isomer-selective two-photon ionization ($2\nu_{UV}$, pump process) from the neutral ground state (S_0, blue surface) to the cationic ground state (D_0, green surface). There, the W molecule migrates from the hydrogen-bonded CO site (AA^+–W^{CO}, left structure, R^+) to the NH-bound isomer (AA^+–W^{NH}, right structure, P^+) by two different pathways. This motion is monitored by TRIR spectra (ν_{IR}) measured at variable delay Δ*t* (probe process). The red trace indicates the fast migration channel with a direct steep descent pathway, and the blue curve illustrates a slow migration channel through a local minimum (I^+). The middle structure illustrates the migration pathways derived from the MD simulations, whereby the red and blue lines indicate the movement of W for the fast and slow channel trajectories, respectively.

---

[*] M. Wohlgemuth, Prof. R. Mitrić
Institut für theoretische und physikalische Chemie
Julius-Maximilians-Universität Würzburg
97074 Würzburg (Germany)
E-mail: roland.mitric@uni-wuerzburg.de

Dr. M. Miyazaki, Dr. M. Weiler, Prof. M. Sakai, Prof. M. Fujii
Chemical Resources Laboratory, Tokyo Institute of Technology
Yokohama 226-8503 (Japan)
E-mail: mfujii@res.titech.ac.jp

Prof. O. Dopfer
Institut für Optik und Atomare Physik
Technische Universität Berlin
10623 Berlin (Germany)
E-mail: dopfer@physik.tu-berlin.de

[**] This study was supported by MEXT (innovative area 2503 Japan), the Core-to-Core Program of JSPS, and the DFG (DO 729/4, ENP-MI-1236).

Supporting information for this article (theory for TRIR spectra based on the MD "on the fly"; computational details; reaction pathways for isomerization; Figures S1 and S2; movies of water motions in representative trajectories of the fast, the slow, and all channels) is available on the WWW under http://dx.doi.org/10.1002/anie.201409047.

important parameters of chemical reactions, but the *structural* time evolution is not probed directly. On the other hand, theoretical approaches to the reaction dynamics treat not only the electronic states but also provide the molecular geometry along the reaction pathway. Thus, molecular dynamics (MD) can give indeed a detailed microscopic picture of the reaction pathways and mechanisms.

The experimental limitations related to probing structural dynamics discussed above may not be a serious problem if only chemical reactions of small molecules such as diatomics are studied, because then the reaction coordinate is simple and straightforward. However, in larger and biologically important molecules and clusters, the reaction and solvation coordinate usually stretches across multidimensional space and is not immediately obvious. To overcome this limit, we present here the fruitful interplay between theoretical simulation and advanced laser spectroscopy, which has the potential to expand the reaction dynamics question indeed from simply "how fast?" to "which way?".[7] Such a step would be analogous to the above-mentioned qualitative advances in the static structural characterization of molecular clusters.

Recently, picosecond pump–probe time-resolved IR (ps TRIR) spectra were reported for probing the migration dynamics of a single water molecule (W) around the CONH peptide linkage in the H-bonded *trans*-acetanilide–water (AA–W) cluster.[8] The TRIR spectra were obtained by combining a two-color tunable ps laser system ($\nu_{UV} + \nu_{IR}$) with appropriate time and spectral resolution (3 ps, 12 cm^{-1}) with a molecular beam time-of-flight mass spectrometer (Figure 1). The solvent molecule W in AA–W^{CO} is initially H-bonded as a proton donor at the CO site in the neutral ground state (S_0). When AA–W^{CO} is resonantly ionized via the first excited state (S_1) to the cationic ground state (D_0) using size- and isomer-selective two-photon ionization ($2\nu_{UV}$, pump process), the interaction potential changes drastically. As

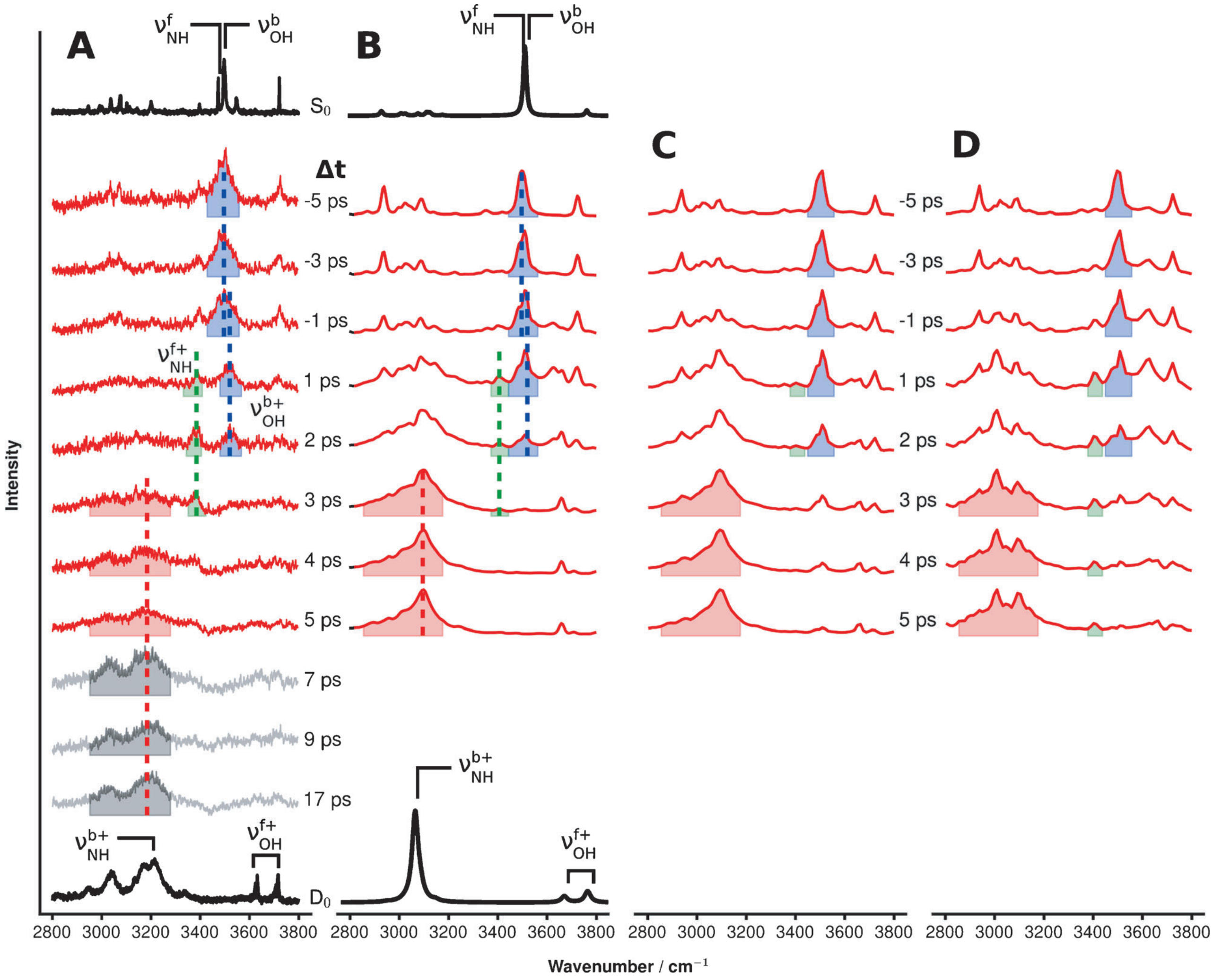

Figure 2. TRIR spectra of AA$^+$–W from the A) ps experiment[8] and B) MD simulations. The S_0 and D_0 spectra are stationary IR spectra of the CO-bound and NH-bound isomers in the neutral and cationic states determined by ns lasers (A) and DFT harmonic frequency calculations for the optimized structures (B). The weak bands at around ν^{f}_{NH} and ν^{b}_{OH} in (A) are combination bands promoted by anharmonic vibrational coupling and thus do not appear in the theoretical spectrum in (B) with harmonic approximations. The highlighted areas indicate the signals uniquely attributed to the NH-bonded isomer (red, P$^+$), the intermediate structure (green, I$^+$) and the CO-bound geometry (blue, R$^+$). The TRIR spectra calculated for trajectories of the fast (C) and slow (D) migration channels are shown separately.

a consequence, W is released from the now repulsive CO site and migrates in an exothermic reaction toward the most attractive NH site. Tunable IR laser radiation (ν_{IR}) introduced at a variable delay Δt after the ionization event probes the isomerization dynamics. Resonant vibrational excitation with ν_{IR} induces the dissociation of the cluster. Thus, the transient IR spectrum can be measured as depletion of the parent cluster ion intensity. The recorded TRIR spectra monitor the W migration in AA$^+$–W in real time by means of the H-bonded OH stretching mode (ν_{OH}^{b+}) of W in the initially formed AA$^+$–W^{CO} cation (reactant R$^+$, blue), the free NH stretching mode (ν_{NH}^{f+}) of the intermediate (I$^+$, green), in which W binds neither to the CO nor the NH site, and the H-bonded NH stretching mode (ν_{NH}^{b+}) of the AA$^+$–W^{NH} reaction product (P$^+$, red). The blue band (R$^+$) disappears within 3 ps, the time needed to release W from the CO site. At the same time, the green band (I$^+$) rises and disappears again at about 5 ps. In parallel, the red band (P$^+$) appears and grows in intensity. These events directly prove that W is released within 3 ps after the ionization and migrates to the NH site via a yet unknown intermediate. Thus, based on these experimental data, the water migration was interpreted as a simple two-step reaction R$^+$→I$^+$→P$^+$, with an overall migration time of 5 ps at an ionization excess energy of $E_{exc} = 9000\ \mathrm{cm}^{-1}$.[8] The time evolution of the three spectral signatures of R$^+$, I$^+$, and P$^+$ are summarized in Figure 3 A. Any P$^+$→I$^+$/R$^+$ back reaction is quenched by efficient intracluster vibrational energy redistribution (IVR), which quickly removes the energy from the reaction coordinate.[8] We note that previous simple MD simulations on the analogous formanilide–W cluster fail to properly reproduce essential features of this reaction, including the time constant, the existence of I$^+$, and the absence of the back reaction.[9]

Although the experimental ps TRIR spectra yield new valuable insight into general reaction parameters (overall time constants, existence of an intermediate), important details of the reaction path (geometry, energetics, barriers) and the competition between multiple possible reaction paths remained unclear.[8] To this end, a sophisticated ab initio MD approach has now been developed to reveal the many more details of the reaction encoded in the highly informative TRIR spectra. To simulate the TRIR spectra, we have carried out “on the fly” MD simulations in the framework of density functional theory and have combined them with the Wigner phase space approach for simulation of the pump–probe spectra.[10] Briefly, the time evolution of the phase space density in the classical limit is described by the Liouville equation $\dot{\rho} = \{H,\rho\}$, where the Hamiltonian function $H = H_0(q,p) - \boldsymbol{\mu}(q)\boldsymbol{\varepsilon}(t)$ is composed of the field-free Hamiltonian H_0 and the interaction with the laser field $\boldsymbol{\varepsilon}(t)$.[11] From the rate of energy absorption $\mathrm{d}\langle E\rangle/\mathrm{d}t$, the total absorption of energy for a given frequency ω and time delay Δt, corresponding to the measured transient TRIR spectrum, has been calculated [Eq. (1)].

$$\begin{aligned}\langle S_{\text{probe}}(\omega,\Delta t)\rangle &= \int_{-\infty}^{\infty} \mathrm{d}t \frac{\mathrm{d}\langle E\rangle}{\mathrm{d}t} = \int_{-\infty}^{\infty}\mathrm{d}t \iint \mathrm{d}\mathbf{q}\mathrm{d}\mathbf{p} H_0\{H,\rho\} \\ &= \sum_{i=1}^{N_{traj}} \int_{-\infty}^{\infty} \mathrm{d}t \frac{\mathrm{d}\boldsymbol{\mu}(\mathbf{q}_i(t))}{\mathrm{d}t}\varepsilon_0 \exp\left(-\frac{(t-\Delta t)^2}{2\sigma^2}\right)\cos\omega t\end{aligned} \tag{1}$$

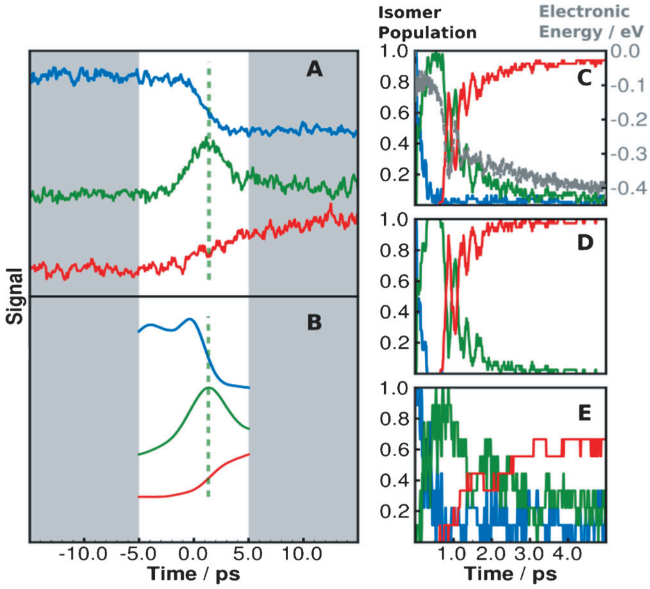

Figure 3. Left: Time evolution of the three vibrational resonances of AA$^+$–W (ν_{OH}^{b+}, ν_{NH}^{f+}, ν_{NH}^{b+}, indicated by blue, green, and red lines in Figure 2 A,B) determined from A) the experimental TRIR spectra[8] and B) the TRIR spectra from the MD simulations. The white area in (A) and (B) indicates the time interval of the MD simulations [−5 ps, +5 ps], and the dashed green lines show the maxima of the I$^+$ signal attributed to the free NH stretch mode in the cationic state (ν_{NH}^{f+}). Right: C) Averaged populations of the total ensemble and the trajectories attributed to D) the fast and E) the slow channels, with the CO-bound isomer (blue, R$^+$), the intermediate structure (green, I$^+$), and the NH-bound isomer (red, P$^+$). The gray dashed line in (C) shows the averaged electronic energy from the MD simulations.

The phase space density has been represented by a discrete set of classical trajectories, which have been propagated in the neutral (S$_0$) and the cationic (D$_0$) states (Figure 4). The electric field of the probe laser pulse is assumed to have a Gaussian shape with the width σ. To take also the pump pulse width into account, the transient TRIR spectra are convoluted by the change in the population of the cationic state $\mathrm{d}P(t)/\mathrm{d}t$, which is derived from the experiment, leading to the expression for the TRIR signal given in Equation (2).

$$\langle S_{\text{pump-probe}}(\omega,\Delta t)\rangle = \int_{-\infty}^{\infty}\mathrm{d}t \langle S_{\text{probe}}(\omega,\Delta t - t)\rangle \frac{\mathrm{d}P(t)}{\mathrm{d}t} \tag{2}$$

As illustrated in Figure 1, we identified two competing mechanisms for the experimentally probed water migration from the initial CO site to the final NH site triggered by photoionization. While in the first channel W migrates along an almost barrierless path across the methyl group (Figure 1, red lines), in the second path W is trapped in a local minimum above the phenyl ring (Figure 1, blue lines). Movies of water motion in representative trajectories of the first and second channels are available in the Supporting Information. The branching ratio for the two paths is 70:30 in favor of the first channel. Figure 3 shows the isomer populations of the first (Figure 3 D) and second process (Figure 3 E) obtained from the MD simulations. The intermediate state, where the CO–W hydrogen bond is already broken, but the NH–W

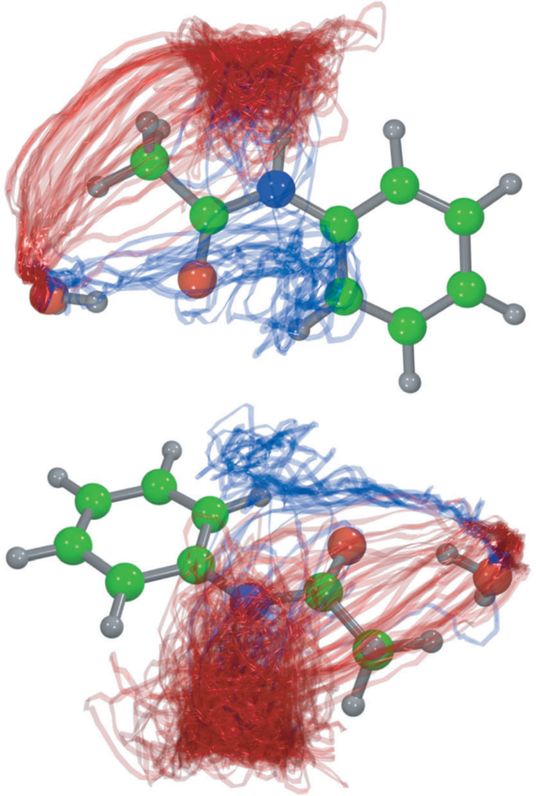

Figure 4. Trajectories obtained from MD simulations in the cationic state shown from two different perspectives. The red and blue curves illustrate the path of the water molecule on migrating from the CO site to the NH site. The blue and red curves are attributed to the slow and fast migration channels, respectively.

hydrogen bond is not yet formed, is reached in both cases within 1 ps. Subsequently, the first path relaxes quickly within further 0.5 ps to the final NH-bound state ("fast channel", Figure 3D), while in the second case complete W transfer is not reached even after 5 ps ("slow channel", Figure 3E). This new two-channel dynamics substantially extends and revises our previous simple one-channel two-step $R^+ \rightarrow I^+ \rightarrow P^+$ mechanism, which was solely derived from the experimental data.[8]

The reliability of the diversity of the reaction pathways predicted by the MD simulations can be tested with high sensitivity by direct comparison between the simulated and measured TRIR spectra (Figure 2). Although the fast channel does not match the initial simple two-step interpretation of the experiment,[8] the simulated TRIR spectra including all trajectories (Figure 2B) well reproduce the observed TRIR spectra (Figure 2A). The TRIR spectra corresponding to the slow channel (Figure 2D), which includes the trapping of W, has a significant intensity for I^+ (green) even at $\Delta t = 5$ ps, whereas the observed TRIR spectra (Figure 2A) do not. This difference clearly indicates that the observed TRIR spectra cannot be reproduced by the slow channel alone, and thus the initial simple two-step model[8] must be revised and extended. Further theoretical and experimental investigations on controlling and directing the reaction by adjusting the excess energy are now in progress.

In conclusion, water migration in AA^+–W includes both slow and fast reaction pathways, and the major channel observed in the ionization experiments is the fast one. It is stressed that this conclusion could only be derived from the direct comparison between the observed and simulated TRIR spectra. In the future, this novel strategy will be used to probe reliably the solvation and reaction dynamics in larger molecular systems such as highly solvated peptides. This approach will thus provide reliable insight into the fundamental mechanisms of various dynamic processes related to solvation at the single-molecule level, and opens the way to controlling the dynamics.

Received: September 15, 2014

Keywords: molecular dynamics · protein hydration · solvation dynamics · time-resolved spectroscopy

---

[1] a) D. H. Levy, *Adv. Chem. Phys.* **1981**, *47*, 323; b) A. W. Castleman, R. G. Keesee, *Acc. Chem. Res.* **1986**, *19*, 413; c) A. W. Castleman, K. H. Bowen, *J. Phys. Chem.* **1996**, *100*, 12911.
[2] S. K. Kim, E. R. Bernstein, *J. Phys. Chem.* **1990**, *94*, 3531.
[3] a) B. Brutschy, *Chem. Rev.* **2000**, *100*, 3891; b) T. Ebata, A. Fujii, N. Mikami, *Int. Rev. Phys. Chem.* **1998**, *17*, 331.
[4] a) A. Fujii, K. Mizuse, *Int. Rev. Phys. Chem.* **2013**, *32*, 266; b) J. A. Fournier, C. J. Johnson, C. T. Wolke, G. H. Weddle, A. B. Wolk, M. A. Johnson, *Science* **2014**, *344*, 1009; c) V. Buch, S. Bauerecker, J. P. Devlin, U. Buck, J. K. Kazimirski, *Int. Rev. Phys. Chem.* **2004**, *23*, 375.
[5] A. Abo-Riziq, L. Grace, E. Nir, M. Kabelac, P. Hobza, M. S. de Vries, *Proc. Natl. Acad. Sci. USA* **2005**, *102*, 20.
[6] a) A. Stolow, J. G. Underwood, *Adv. Chem. Phys.* **2008**, *139*, 497; b) A. Stolow, A. E. Bragg, D. M. Neumark, *Chem. Rev.* **2004**, *104*, 1719; c) D. M. Neumark, *Annu. Rev. Phys. Chem.* **2001**, *52*, 255; d) T. Suzuki, *Annu. Rev. Phys. Chem.* **2006**, *57*, 555.
[7] a) S. Takeuchi, S. Ruhman, T. Tsuneda, M. Chiba, T. Taketsugu, T. Tahara, *Science* **2008**, *322*, 1073; b) D. A. Blank, *Science* **2008**, *322*, 1056.
[8] K. Tanabe, M. Miyazaki, M. Schmies, A. Patzer, M. Schütz, H. Sekiya, M. Sakai, O. Dopfer, M. Fujii, *Angew. Chem. Int. Ed.* **2012**, *51*, 6604; *Angew. Chem.* **2012**, *124*, 6708.
[9] a) H. Tachikawa, M. Igarashi, T. Ishibashi, *J. Phys. Chem. A* **2003**, *107*, 7505; b) T. Ikeda, K. Sakota, Y. Kawashima, S. Yuiga, H. Sekiya, *J. Phys. Chem. A* **2012**, *116*, 3816.
[10] V. Bonačić-Koutecký, R. Mitrić, *Chem. Rev.* **2005**, *105*, 11.
[11] R. Mitrić, V. Bonačić-Koutecký, *Phys. Rev. A* **2007**, *76*, 031405.
[12] J. P. Perdew, K. Burke, M. Ernzerhof, *Phys. Rev. Lett.* **1996**, *77*, 3865.
[13] R. Krishnan, J. S. Binkley, R. Seeger, J. A. Pople, *J. Chem. Phys.* **1980**, *72*, 650.
[14] S. Grimme, *J. Comput. Chem.* **2004**, *25*, 1463.
[15] W. C. Swope, H. C. Andersen, P. H. Berens, K. R. Wilson, *J. Chem. Phys.* **1982**, *76*, 637.
[16] a) H. Jónsson, G. Mills, K. W. Jacobsen in *Classical and Quantum Dynamics in Condensed Phase Simulations* (Eds.: B. J. Berne, G. Ciccotti, D. F. Coker), World Scientific, Singapore, **1998**, p. 385; b) G. Henkelman, H. Jónsson, *J. Chem. Phys.* **1999**, *111*, 7010; c) G. Henkelman, G. Jóhannesson, H. Jónsson in *Progress on Theoretical Chemistry and Physics* (Ed.: S. D. Schwartz), Kluwer, Dordrecht, **2000**, p. 269; d) D. Sheppard, R. Terrell, G. Henkelman, *J. Chem. Phys.* **2008**, *128*, 134106.